Ionospheric Signatures of Plasmaspheric Tails

J. C. Foster, P. J. Erickson, A. J. Coster, J. Goldstein, and F. J. Rich

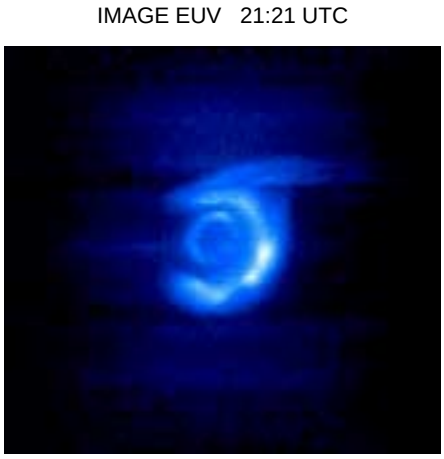

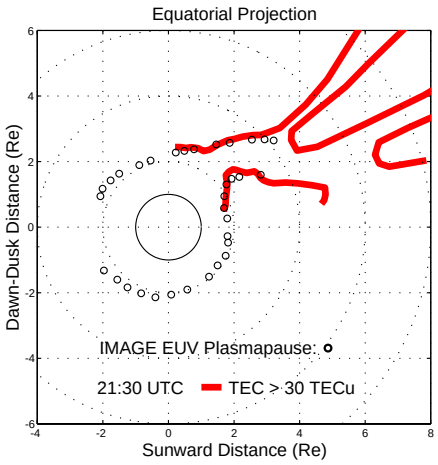

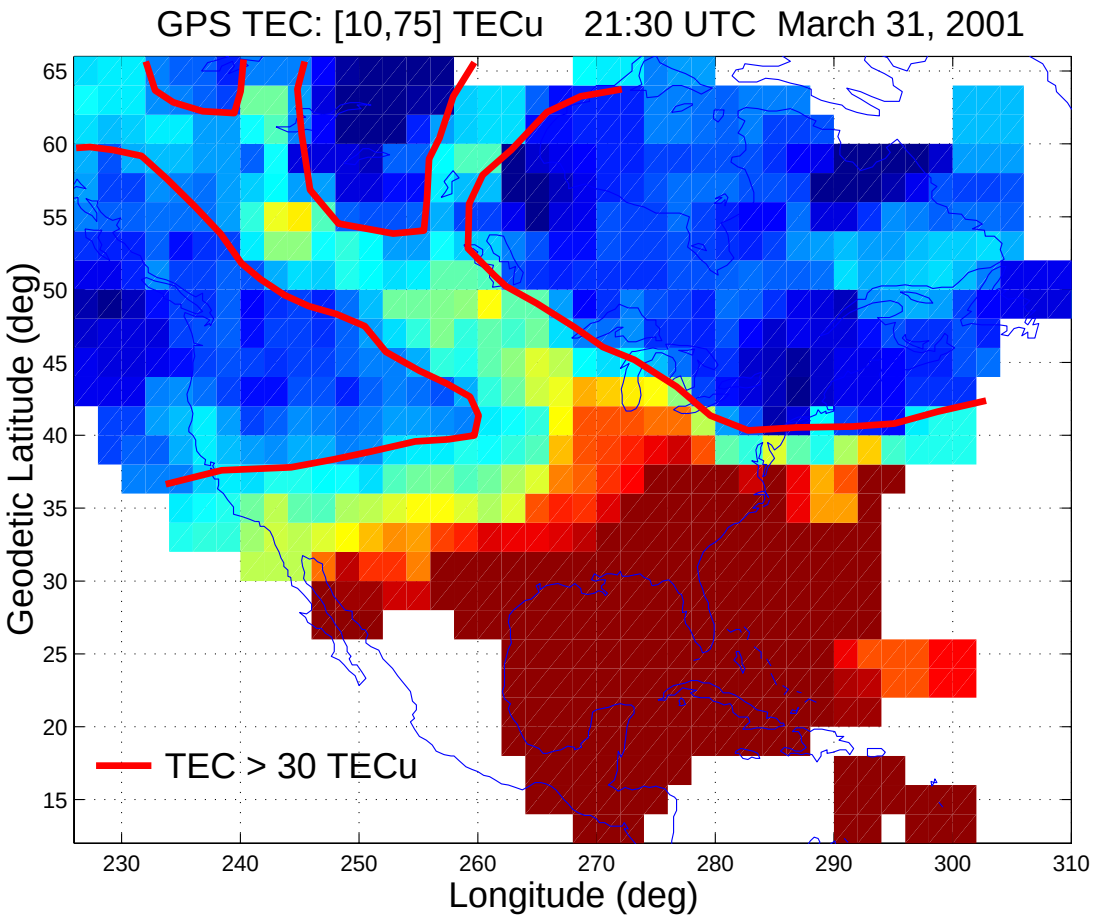

[Foster, J. C., P. J. Erickson, A. J. Coster, J. Goldstein, and F. J. Rich, Ionospheric signatures of plasmaspheric tails, *Geophys. Res. Lett., 29*(13), 10.1029/2002GL015067, 2002.]

Cover:
(top left) Space-based IMAGE EUV observations of Earth's plasmasphere reveal a sunward-directed plasmatail (image courtesy B. Sandel).
(top right) Circles denote the plasmapause position scaled from the EUV imagery. Superimposed in red is the equatorial-plane projection of the >30 TECU boundary determined from ground-based GPS observations.
(bottom) GPS navigation signals monitored at >120 sites are analyzed to provide a snapshot of ionospheric total electron content (TEC) over North America during the major geomagnetic storm of 31 March 2001. A large-scale plume of storm enhanced density (SED) spans the continent from a source region in the eastern US. The bold contour at TEC > 30 units outlines the low-altitude footprint of the TEC plume which maps directly into the plasmaspheric tail observed by IMAGE EUV (see Foster et al., this issue).

Ionospheric Signatures of Plasmaspheric Tails

J. C. Foster and P. J. Erickson

MIT Haystack Observatory, Westford, Massachusetts

A. J. Coster

MIT Lincoln Laboratory, Lexington, Massachusetts

J. Goldstein

Rice University, Houston, Texas

F. J. Rich

Air Force Research Laboratory, Hanscom AFB, Massachusetts

Abstract. We make direct comparisons between GPS maps of total electron content (TEC) over the North American continent, Millstone Hill radar observations of storm enhanced density, and low and high-altitude satellite measurements of the perturbation of the outer plasmasphere during the March 31, 2001 geomagnetic storm. We find that storm enhanced density (SED) and plumes of greatly-elevated TEC are associated with the erosion of the outer plasmasphere by strong sub-auroral polarization electric fields. The SED/TEC plumes identified at low altitude map closely onto the magnetospheric determination of the boundaries of the plasmapause and plasmaspheric tail determined by EUV imaging from the IMAGE spacecraft. Characteristics of the SED/TEC plumes/tails for the March 31, 2001 event are: TEC ~ 100 TECu; *F*- region sunward velocity ~ 1000 m/s; sunward flux ~$5*10^{24}$ ions s^{-1}; total transport to dayside magnetopause/merging region (3-hr event) ~$5*10^{28}$ ions.

1. Introduction

Severe space weather effects have been observed at mid latitudes over the continental US during the strong magnetic storms of the current solar cycle. Large-scale enhancements of total electron content (TEC), steep spatial gradients in ionospheric plasma parameters and TEC [*Vo and Foster*, 2001], and the occurrence of strong radio scintillation occur in the sub-auroral region which usually is free from such disturbances. This study reports a coordinated investigation of such events using ground-based GPS, incoherent scatter radar, and low and high-altitude satellite observations. We find a direct relationship between sub-auroral ionospheric perturbations and the structuring and dynamics of the overlying plasmasphere.

A number of important magnetospheric boundaries are found near the auroral/sub-auroral transition, nominally near 60˚ invariant latitude (Λ), and these result in the ionospheric structure and dynamics which characterize the local ionospheric observations made from MIT's Millstone Hill Observatory, located near 54˚ Λ in eastern Massachusetts. The high-altitude plasmapause [*Carpenter*, 1963] maps down to the region near the equatorward edge of the (mid-latitude) ionospheric trough (e.g. *Foster et al*. [1978]) and is associated with the transition between the co-rotating inner magnetosphere and the convection-driven ionospheric circulation at auroral latitudes. As the level of geomagnetic disturbance increases, the electric fields and particle populations which characterize the auroral region expand equatorward and their effects are felt at sub-auroral latitudes.

1.1 Storm Enhanced Density

The Millstone Hill incoherent scatter radar frequently observes storm enhanced density (SED) in the pre-midnight sub-auroral ionosphere during the early stages of magnetic storms [*Foster*, 1993]. These high-TEC plumes of ionization appear near the equatorward edge of the mid-latitude ionospheric trough, convecting sunward, driven by poleward-directed electric fields.

Figure 1 presents observations of SED during Kp ~6 conditions (after *Foster* [1993]). This MLT/latitude map was built up from Millstone Hill incoherent scatter radar scans taken over a 24-hour period. Storm enhanced density appears in the post-noon sector in the region poleward of the regular diurnal solar enhancement of the topside *F* region. SED was seen continuously by the radar for > 8 hours during this event. *Su et al.* [2001] mapped these low-altitude observations to the equatorial plane of the magnetosphere and found that the SED feature mapped into a dayside plume of sunward-streaming plasmaspheric materials observed at geosynchronous orbit (a plasmasphere drainage plume [*Elphic et al*., 1996]). That study concluded that SED is an ionospheric signature of the erosion of the outer

plasmasphere which traces the path of plasmaspheric materials as they are swept to the dayside magnetopause/merging region [*Elphic et al*., 1997].

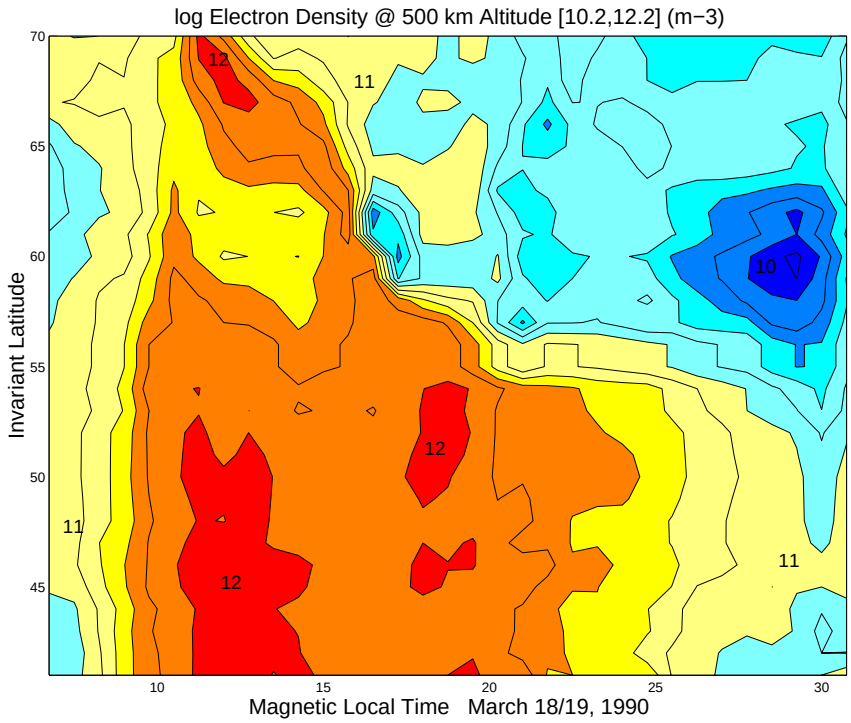

Figure 1. Storm enhanced density observed with the Millstone Hill incoherent scatter radar is seen as a tongue of ionization extending poleward and toward noon from the afternoon sector mid- latitude ionosphere (after *Foster* [1993]).

1.2 Sub-Auroral Polarization Electric Field

Strong polarization electric fields develop across the sub-auroral ionosphere during disturbed conditions (e.g. *Yeh et al.* [1991]). Field aligned currents driven by hot plasma pressure gradients in the inner magnetosphere close across the sub-auroral ionosphere [e.g. *Liemohn et al*., 2001]. On the night side, in the absence of particle precipitation, these currents flow across regions of low ionospheric conductivity. Enhanced ionospheric recombination occurs due to the increasing sub-auroral electric field [*Schunk et al*., 1976], resulting in the formation of a deep ionospheric trough. In the presence of reduced ionospheric conductance, the electric field across the region rises, and the sub-auroral polarization stream (SAPS) is formed.

Statistical observations of SAPS with the Millstone Hill radar [*Foster and Vo*, 2002] indicate that this broad, persistent region of ring-current induced electric field can be seen equatorward of the two-cell convection, across the night sector to dawn. The SAPS electric field is strongest near 22 MLT, where it often abuts and overlaps the high- TEC region of the outer plasmasphere.

1.3 Plasmaspheric Tails

Early observations of thermal ion species and fluxes in the inner magnetosphere identified cases of a double plasmapause in the evening sector [*Chappell*, 1974]. These observations were interpreted in terms of detached plasmaspheric regions or plasma tails, attached to the main plasmasphere, but stretching outward and sunward under the influence of electric field-driven convection [*Chen and Grebowsky*, 1974]. *Carpenter et al*. [1993] present a detailed description of the observations and characteristics of the plasmaspheric bulge and detached plasma region. An exciting recent capability is the direct observation of the extent and dynamics of the plasmasphere by the IMAGE satellite [*Sandel et al*., 2000; 2001]. EUV images using resonantly-scattered sunlight from plasmaspheric helium depict the structure and evolution of the plasmapause across wide swaths of MLT. For the first time, plasmaspheric tails are seen stretching sunward from the perturbed afternoon-sector plasmasphere. In the analysis presented below, plasmapause/ tail boundaries have been scaled and projected into MLT/*L*-shell coordinates for each EUV image over a 7-hour interval, depict-

ing the extent and dynamics of these major perturbations of the inner magnetosphere's thermal plasma environment.

2. Observations: March 31, 2001 Storm

We make direct comparisons between GPS maps of total electron content (TEC) over the North American continent, Millstone Hill radar observations of storm enhanced density, and low and high-altitude satellite measurements of the perturbation of the outer plasmasphere during the March 31, 2001 geomagnetic storm (Kp = 9). During this event we have simultaneous DMSP satellite and Millstone Hill radar observations to further define the SED/plasmatail characteristics.

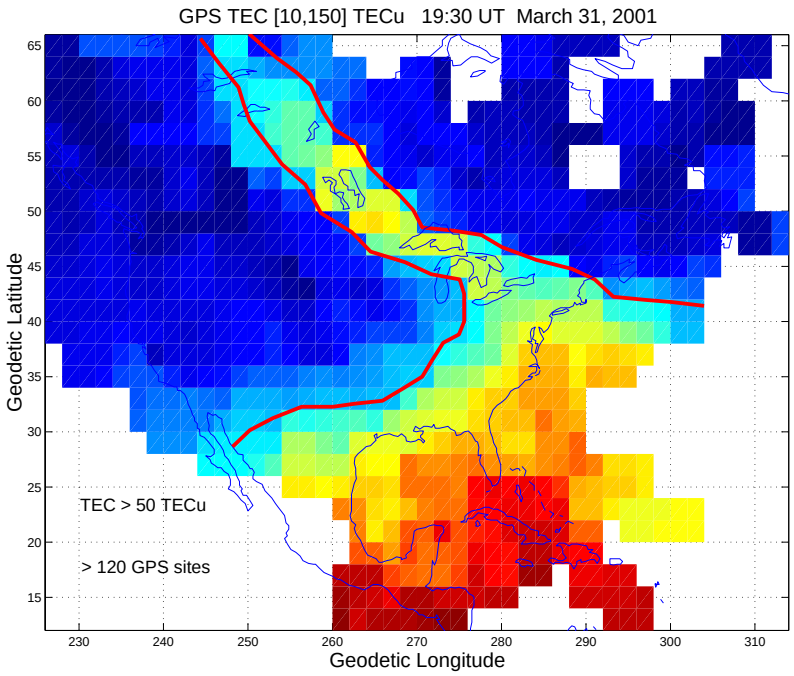

Figure 2. Snapshot of SED plume in the post-noon sector obtained by plotting vertical TEC obtained from > 120 GPS receiving sites during a 15-min interval. The 50 TECu contour is outlined in red and defines the instantaneous position of the SED/TEC enhancement.

2.1 GPS Maps of Total Electron Content

The satellites of the GPS constellation are in 12-hr circular orbits (~20,000-km altitude) with orbital inclination ~55˚. Data from a global network of GPS receivers are accessible via the SOPAC data archive on the World Wide Web (http://sopac.ucsd.edu). TEC can be determined along the paths from each receiver to the GPS satellites in view (typically 6-12). *Coster et al*. [1990] have investigated the characteristics of GPS TEC and have compared and calibrated these with profiles of *F*-region ionospheric densities determined from the co-located Millstone Hill radar site. This work showed early evidence of the plasmaspheric contribution to the GPS TEC measurements.

We have calculated vertical TEC from > 120 GPS sites in North America and the Caribbean using the standard ionospheric mapping function [*Coster et al*., 1992]. Biases were removed and maps of TEC over the North American continent were prepared at 15-min intervals. Figure 2 presents a GPS TEC map for 19:30 UT on March 31, 2001. Determinations of vertical TEC have been binned in 2˚x2˚ latitude/longitude bins and color coded between 10 and 150 TEC units (one TECu = 10^{16} electrons m^{-2}). No smoothing is used and the large number of ionospheric pierce points included in each frame (~10,000) produces a high level of detail. A pronounced band of storm enhanced density extends from the New England coast across the Great Lakes region and into central Canada. This snapshot of the TEC plume is qualitatively

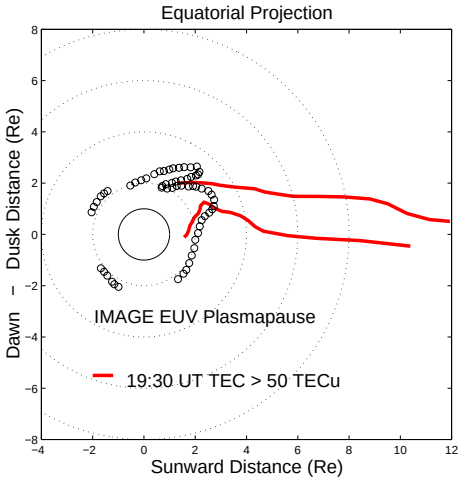

Figure 3. The 50 TECu boundary of the SED plume shown in Figure 2 is mapped into the equatorial plane (dipole mapping). Simultaneous location of the plasmapause boundary determined from IMAGE EUV is shown by circles. The SED plume maps into an extended plasmaspheric tail.

similar to the composite picture of SED shown in Figure 1.

A red line marks the 50 TECu contour which outlines the ionospheric plume. In Figure 3 this contour has been mapped into the equatorial plane of the magnetosphere using a simple dipole-field mapping, assuming no distortion of the dayside magnetic field. The ionospheric SED plume maps into an extended plasmaspheric tail stretching toward the noontime magnetopause. Circles denote the simultaneous determination of the plasmasphere boundary scaled from the corresponding IMAGE EUV frame. IMAGE observed a highly eroded plasmasphere with plasmapause near L=2 and the formation of a plasmaspheric tail co-located with the projected position of the SED/TEC plume. The ground-based observations provide rich detail which complements the direct plasmasphere imagery. A further example of the excellent co-location of these features found throughout this event is shown on the cover of this issue.

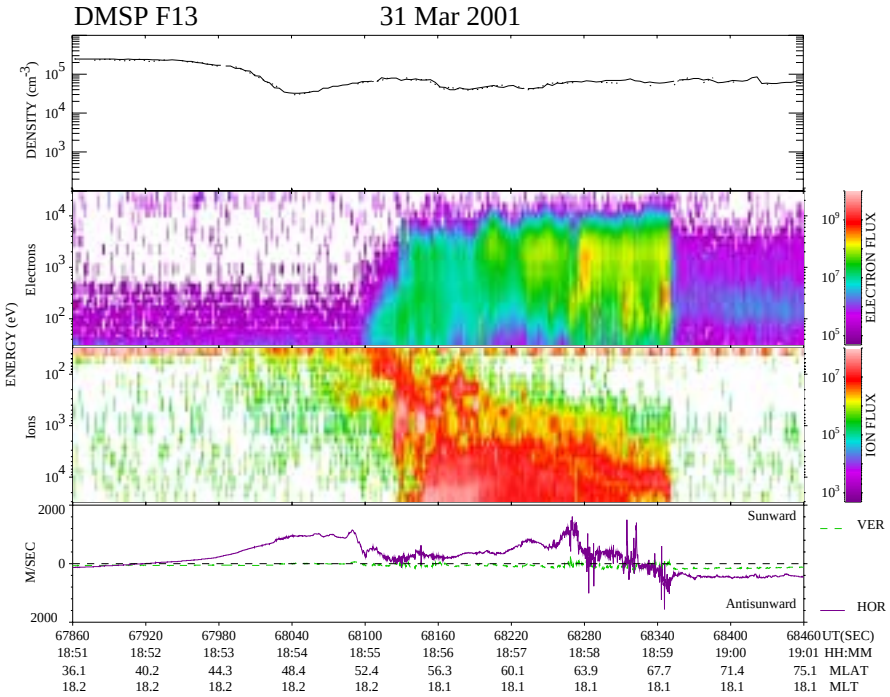

Figure 4. As DMSP F13 crossed the SED plume, SAPS sunward ion convection (IDM, lower trace) was seen near 50˚Λ in the low-conductance region equatorward of the auroral precipitation (middle plots). The SED plume is formed in the region 45˚-48˚Λ, where the SAPS overlaps the outer plasmasphere /equatorward trough boundary (RPA data, top trace.)

2.2 Low-Altitude Boundaries

DMSP satellites circle the earth in sun-synchronous dawn-dusk orbits at ~900 km altitude. DMSP F13 flew over the region of the SED/TEC plume near 19:00 UT. Ion drift meter observations shown in Figure 4 identify SAPS sunward ion velocity ~1000 m/s over a wide band of latitudes from 45˚ - 52˚ Λ. The sub-auroral convection peak spans the ionospheric trough seen in the RPA density data, and lies entirely equatorward of the low-latitude boundary of plasma sheet electron precipitation at ~53˚ Λ. The equatorward portion of the SAPS convection overlaps the poleward edge of elevated (plasmaspheric) density between 45˚ - 48˚ Λ. Here, ion velocities of 500 - 1000 m/s drive a sunward ion flux of ~10^{15} ions $m^{-2}s^{-1}$. The SED/TEC plume/plasma tail is formed in this overlap region.

2.3 Radar Observations of Sunward Flux

The Millstone Hill incoherent scatter radar observed high speed sunward ion convection associated with the SAPS in the post-noon sector. A deep ionospheric trough was formed coincident with the peak of the SAPS electric field. Sunward ion flux was greatly enhanced at the equatorward extent of the region of rapid ion convection, where the SAPS electric fields overlapped the equatorward edge of the trough. In Figure 5 we present a 2-D map of radar observations of sunward ion flux at 19:10 UT, determined as the product of density and velocity. The color scale spans two orders of magnitude, reaching ~10^{15} ions $m^{-2}s^{-1}$ in the center of the flux channel. The superimposed 50 TECu contours of

Figure 2 indicate that the ionospheric TEC/SED plume was convecting sunward (i.e. along the plume) at speeds >1000 m/s.

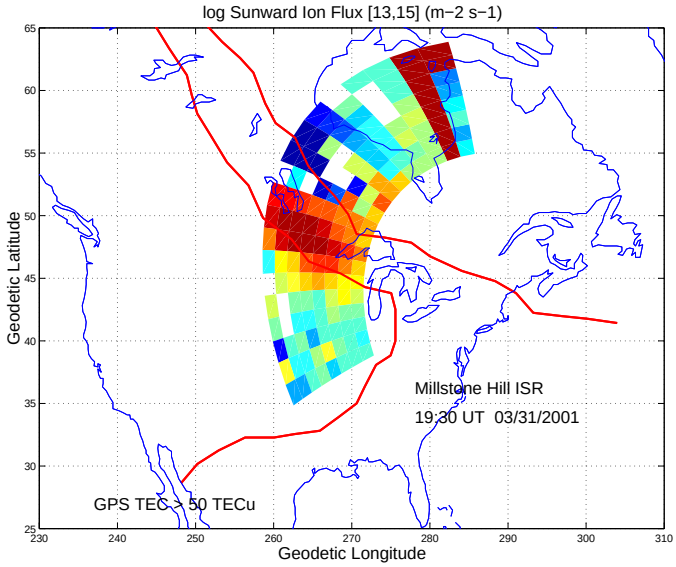

Figure 5. Intense sunward ion flux (density x velocity) was observed with Millstone Hill radar azimuth scans across the region of the SED plume. Ion flux ~10^{15} $m^{-2}s^{-1}$ was observed coincident with the GPS TEC/SED feature of Figure 2.

Detailed radar observations of plasma velocity and density across the SED plume are presented in Figure 6. In this early post-noon sector, the two regions of SAPS and auroral sunward convection have merged at a somewhat higher magnetic latitude than seen at the later local time of the DMSP pass of Figure 4. For this observation at ~14 MLT, the SAPS convection extends some 10˚ into the high-density region of the plasmasphere/plasma-tail, whose low-altitude footprint constitutes the equatorward wall of the ionospheric trough.

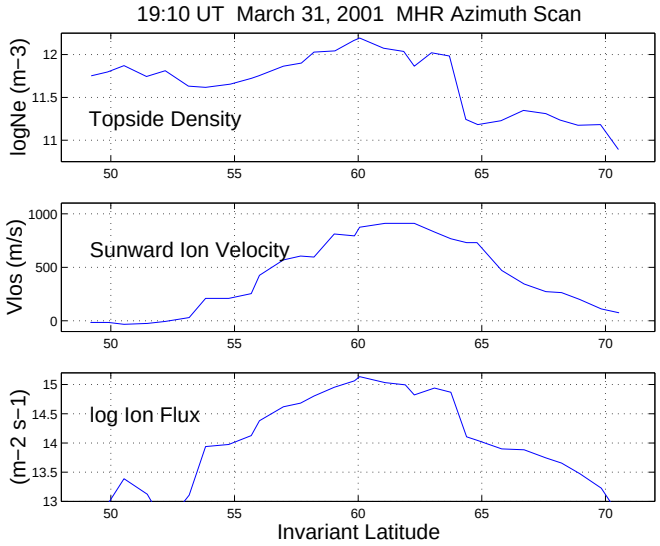

Figure 6. Topside *F*-region ion density (top), velocity (middle), and sunward flux (bottom) derived from the radar azimuth scan shown in Figure 5. Ion flux exceeds 10^{15} ions $m^{-2}s^{-1}$ at L=4 in the ionospheric footprint of the plasmaspheric tail.

Characteristics observed in the SED/tail plume for this event are as follows. TEC (from GPS) was 50 - 100 TECu. *F*-region (300 km -1000 km altitude) sunward velocity ranged from 500 m/s - 1000 m/s. Sunward flux, determined as the product of TEC and *F*-region sunward velocity over 3˚ latitude, was ~$5*10^{24}$ ions s^{-1}. Total transport to the dayside magnetopause/merging region over the course of the 3-hr event was ~$5*10^{28}$ ions.

3. Discussion

In this event we find that storm enhanced density results from the erosion of the outer plasmasphere by the sub-auroral polarization stream electric field and that the SED/TEC plumes seen in the ionosphere map directly into the dramatic plasmaspheric tails which are depicted in the IMAGE EUV images. Our observations indicate a near-circu-

lar night-sector configuration and a highly-eroded position (near L=2) for the plasmapause in this highly disturbed event.

The excellent comparison between Figures 1 and 2 indicates that the SED/plasmatail can be a long-lived phenomenon, roughly fixed in local time, such that the scanning radar, fixed to the earth, rotates under it from noon to dusk. The SED maps presented by *Foster* [1993] present pictures of the footprints of long-lived plasmaspheric tails, and the characteristics of the SED events reported in that earlier study provide a detailed description of the ionospheric signatures of this plasmaspheric phenomenon.

Acknowledgements. IMAGE EUV images and analysis software were provided by B. Sandel. This work is partially sponsored by the Air Force under Air Force Contract AF19628-00-C-0002. Opinions, interpretations, conclusions, and recommendations are those of the authors and are not necessarily endorsed by the United States Air Force. The Millstone Hill Observatory is supported by a Co-operative Agreement between the National Science Foundation and the Massachusetts Institute of Technology.

References

Carpenter, D. L., Whistler evidence of a 'knee' in the magnetospheric ionization density profile, *J. Geophys. Res., 68*, 1675, 1963

Carpenter, D. L., B. L. Giles, C. R. Chappell, P. M. E., Decreau, R. R. Anderson, A. M. Persoon, A. J. Smith, Y. Corcuff, and P. Canu, Plasmaspheric dynamics in the duskside bulge region: a new look at an old topic, *J. Geophys. Res., 98*, 19243, 1993.

Chappell, C. R., Detached plasma regions in the magnetosphere, *J. Geophys. Res., 79*, 1861, 1974.

Chen, A. J., and J. M. Grebowsky, Plasma tail interpretations of pronounced detached plasma regions measured by OGO 5, *J. Geophys. Res., 79*, 3851, 1974.

Coster, A. J., E. M. Gaposchkin, L. E. Thornton, M. Buonsanto, and D. Tetenbaum, Comparison of GPS and Incoherent Scatter Measurements of the Total Electron Content, *The Effect of the Ionosphere on Radiowave Signals and System Performance,* 460-469, 1990.

Coster, A. J., E. M. Gaposchkin, and L. E. Thornton, Real-Time Ionospheric Monitoring System Using GPS, *Navigation, 39, 2*, 1992.

Elphic, R. C., L. A. Weiss, M. F. Thomsen, D. J. McComas, and M. B. Moldwin, Evolution of plasmaspheric ions at geosynchronous orbit during times of high geomagnetic activity, *Geophys. Res. Lett., 23*, 2189, 1996.

Elphic, R. C., M. F. Thomsen, and J. E. Borovsky, The fate of the outer plasmasphere, *Geophys. Res. Lett., 24*, 365, 1997.

Foster, J. C., Storm-Time Plasma Transport at Middle and High Latitudes*, J. Geophys. Res., 98,* 1675-1689. 1993.

Foster, J. C., C. G. Park, L. H. Brace, J. R. Burrows, J. H. Hoffman, E. J. Maier, J. H. Whittaker, Plasmapause signatures in the ionosphere and magnetosphere, *J. Geophys. Res., 83,* 1175, 1978.

Foster, J. C., and H. B. Vo, Activity Dependence of Sub-Auroral Electric Fields, *Geophys. Res. Lett.,* submitted, 2002.

Liemohn, M. W., J. U. Kozyra, C. R.Clauer, and A. J. Ridley, Computational analysis of the near- Earth magnetospheric current system during two-phase decay storms, *J. Geophys. Res., 106*, 29531, 2001.

Sandel, B. R., et al., The extreme ultraviolet imager investigation for the IMAGE mission, *Space Sci. Rev., 91*, 197, 2000.

Sandel, B. R., et al., Initial Results from the IMAGE Extreme Ultraviolet Imager, *Geophys. Res. Lett., 28*, 1439, 2001.

Schunk, R. W., P. M. Banks, and W. J. Raitt, Effects of electric fields and other processes upon the nighttime high-latitude *F* layer, *J. Geophys. Res., 80*, 3121, 1976.

Su, Y.-J., M. F. Thomsen, J. E. Borovsky, and J. C. Foster, A linkage between polar patches and plasmaspheric drainage plumes, *Geophys. Res. Lett., 28*, 111, 2001.

Vo, H. B, and J. C. Foster, A Quantitative Study of Ionospheric Density Gradients at Mid-Latitudes, *J. Geophys. Res. 106*, 21555, 2001.

Yeh, H.-C., J. C. Foster, F. J. Rich, and W. Swider, Storm-time electric field penetration observed at mid-latitude, *J. Geophys. Res., 96*, 5707, 1991.